

INVESTIGATION OF MONOPOLE MODES AND FREQUENCY ERRORS WITH AN EXTENDED CIRCUIT MODEL IN 3.9 GHz CAVITIES FOR FLASH/XFEL

B. Szczesny

The University of Manchester, Manchester M13 9PL, UK
Cockcroft Institute of Science and Technology, Daresbury, Cheshire WA4 4AD, UK

Abstract

Monopole modes in the first eight bands of a single cell and a 9-cell accelerating structure of 3.9 GHz cavities were analysed in computer simulations. The circuit model was extended to include next nearest neighbour in addition to nearest neighbour coupling. This enables an accurate analytical characterisation of dispersion curves for higher order monopole bands. The effects of frequency errors on field flatness were simulated using circuit model. It was demonstrated that these can be reduced by tuning only the end cells of the structure.

The compensation follows from a Fourier expansion of a square wave. The first term in the infinite series is the fundamental mode and the second term is the 3.9 GHz third harmonic with a coefficient of a third

$$E(\phi)/E_0 \approx \sin(\phi) + \frac{1}{3} \sin(3\phi).$$

However, to ensure that the second derivative of the field is zero at the peak of the field, the coefficient of the third harmonic is set to a ninth (see Fig. 1). [2]

1. INTRODUCTION

The accelerating field of the 1.3 GHz cavity has a cosine-like dependence. As a result, electrons experience a varying force and consequently there is a significant energy spread across the bunch. Therefore, to minimise the energy spread the accelerating field should not vary across the bunch. A significant linearisation of the RF curvature can be achieved with a 3.9 GHz cavity. [1]

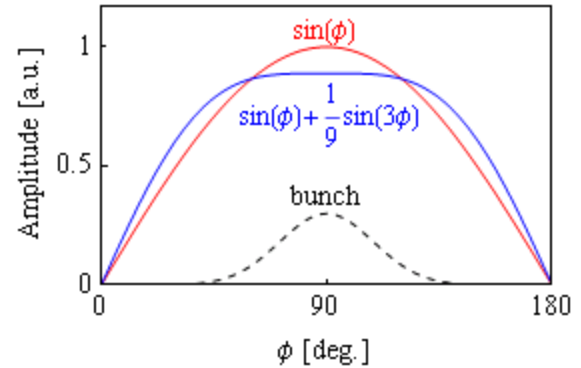


Figure 1: Linearisation of RF curvature.

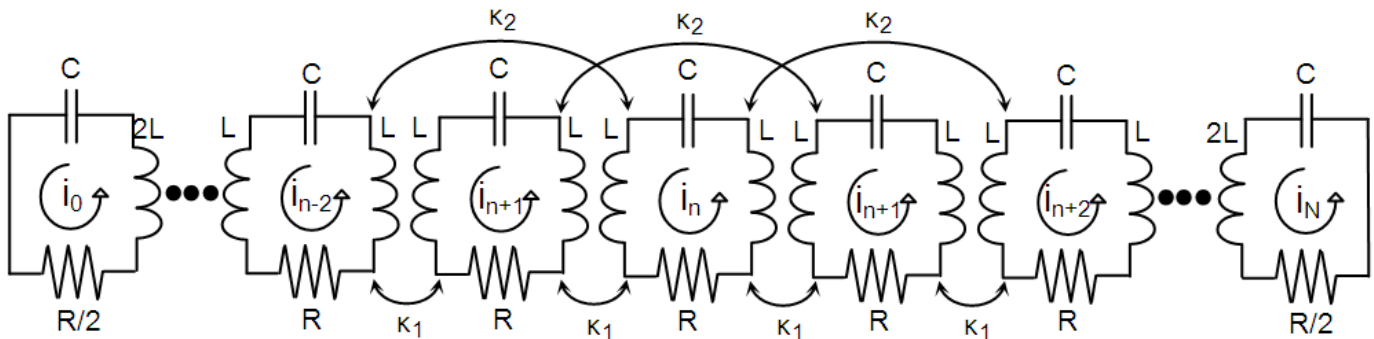


Figure 2: Circuit model of the monopole modes of coupled resonant cells.

2. THEORY

2.1 Extended Circuit Model

A circuit model can be employed to analyse excited resonant modes of a linear array of coupled cavities. Individual cells are represented as a circuit consisting of inductors, capacitors and resistors with currents replacing fields. An inductive coupling represents interaction of the fields between nearest neighbours and it is set proportional to a coupling constant κ_1 . Similarly, next nearest neighbour coupling is proportional to κ_2 . The end cavities are half-cells with twice the inductance of the mid cell to ensure equal resonant frequencies and half the resistance (see Fig. 2). Summing voltages around each circuit gives a following system of equations

$$i_0 \left(j\omega L + \frac{1}{2j\omega C} + \frac{R}{2} \right) + j\omega \kappa_1 L i_1 + j\omega \kappa_2 L i_2 = 0$$

$$i_n \left(2j\omega L + \frac{1}{j\omega C} + R \right) + j\omega \kappa_1 L (i_{n-1} + i_{n+1}) + j\omega \kappa_2 L (i_{n-2} + i_{n+2}) = 0$$

$$i_N \left(j\omega L + \frac{1}{2j\omega C} + \frac{R}{2} \right) + j\omega \kappa_1 L i_{N-1} + j\omega \kappa_2 L i_{N-2} = 0$$

multiplying by $1/j\omega L$ and defining

$$\omega_0^2 = \frac{1}{2LC}; \quad Q = \frac{2\omega_0' L}{R}$$

$$\omega_0^2 = \omega_0'^2 \left(1 + j \frac{\omega}{\omega_0} \frac{1}{Q} \right) \Big|_{Q \sim 10^{10}} \approx \omega_0'^2$$

allows the following simplification

$$i_0 \left(1 - \frac{\omega_0^2}{\omega^2} \right) + \kappa_1 (i_1) + \kappa_2 (i_2) = 0$$

$$i_n \left(1 - \frac{\omega_0^2}{\omega^2} \right) + \frac{\kappa_1}{2} (i_{n-1} + i_{n+1}) + \frac{\kappa_2}{2} (i_{n-2} + i_{n+2}) = 0$$

$$i_N \left(1 - \frac{\omega_0^2}{\omega^2} \right) + \kappa_1 (i_{N-1}) + \kappa_2 (i_{N-2}) = 0$$

and this forms a circuit model eigensystem

$$\begin{pmatrix} 1 & \kappa_1 & \kappa_2 & 0 & \dots & 0 \\ \kappa_1/2 & 1 & \kappa_1/2 & \kappa_2/2 & & \vdots \\ \kappa_2/2 & \kappa_1/2 & 1 & \kappa_1/2 & & \vdots \\ 0 & & & \ddots & & 0 \\ \vdots & & & & \kappa_1/2 & 1 & \kappa_1/2 \\ 0 & \dots & 0 & \kappa_2 & \kappa_1 & 1 \end{pmatrix} \begin{pmatrix} i_0 \\ i_1 \\ \vdots \\ i_n \\ \vdots \\ i_N \end{pmatrix} = \frac{\omega_0^2}{\omega^2} \begin{pmatrix} i_0 \\ i_1 \\ \vdots \\ i_n \\ \vdots \\ i_N \end{pmatrix}$$

$$\Rightarrow \underline{\underline{M}} i = \frac{\omega_0^2}{\omega^2} i.$$

In order to find normal modes, $\underline{\underline{M}}$ is solved to give $N+1$ eigenvalues and eigenvectors representing resonant frequencies and field distributions respectively. As previously indicated, the imaginary part of the angular frequency can be approximated as zero since Q values of superconducting cavities are very high, in order of 10^{10} .

The equation for a middle cell can be simplified by considering an infinite periodic chain of cavities without end cells. Assuming a Floquet condition of constant phase advance ϕ across one cell and current variation of $e^{-j\omega t}$ gives

$$i_{n+1} e^{-j\omega t} = i_n e^{-j\omega t} e^{\pm j\phi} \Rightarrow$$

$$i_n e^{-j\omega t} \left(1 - \frac{\omega_0^2}{\omega^2} \right) + \frac{\kappa_1}{2} i_n e^{-j\omega t} (e^{-j\phi} + e^{+j\phi})$$

$$+ \frac{\kappa_2}{2} i_n e^{-j\omega t} (e^{-2j\phi} + e^{+2j\phi}) = 0$$

which after cancelling $i_n e^{-j\omega t}$ and converting complex exponentials into cosines becomes

$$\omega = \frac{\omega_0}{\sqrt{1 + \kappa_1 \cos \phi + \kappa_2 \cos 2\phi}}$$

an equation describing a dispersion curve for an infinite chain of coupled cavities. It also provides an accurate description for a finite chain but adding end cells and beam pipes results in discrepancies. The equation can be solved to obtain the resonant frequency and the coupling constants by substituting frequencies and phases of modes found in simulations.

2.2 Classical Circuit Model

It can be shown that the extended form is consistent with classical results from the circuit model with only the next nearest neighbour coupling. [3, 4, 5] In the case of vanishing κ_2 the dispersion curve equation reduces to

$$\omega = \frac{\omega_0}{\sqrt{1 + \kappa_1 \cos \phi}}$$

2.3 Frequency errors

In order to investigate the effects of frequency errors due to imperfection in manufactured cavities, each cell was assigned its own resonant frequency. This means that one can no longer factorise ω_0 out of the matrix in the eigensystem

$$\begin{pmatrix} 1/\omega_0^2 & \kappa_1/\omega_0^2 & & & & \\ \kappa_1/2\omega_1^2 & 1/\omega_1^2 & & & & \\ & & \ddots & & & \\ & & & 1/\omega_9^2 & \kappa_1/2\omega_9^2 & \\ & & & \kappa_1/\omega_{10}^2 & 1/\omega_{10}^2 & \\ & & & & & \ddots \end{pmatrix} \begin{pmatrix} i_0 \\ \vdots \\ i_n \\ \vdots \\ i_N \end{pmatrix} = \frac{1}{\omega^2} \begin{pmatrix} i_0 \\ \vdots \\ i_n \\ \vdots \\ i_N \end{pmatrix}$$

The resulting eigenvectors now have different components which means that the field in the structure is not flat. The field flatness was defined as

$$FF = \left(1 - \frac{\sigma}{\mu}\right) \times 100\%$$

where μ is the mean of the eigenvector components and σ is a corresponding standard deviation.

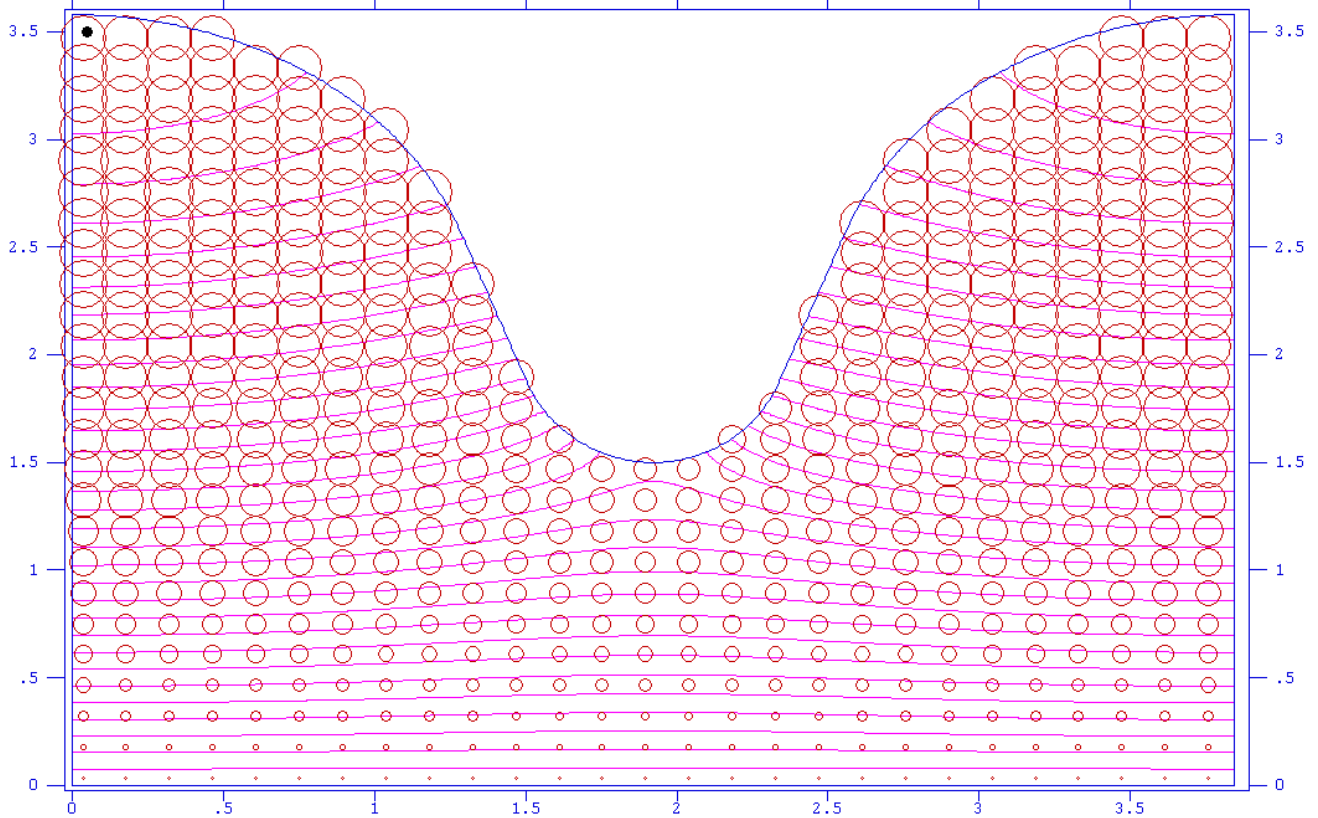
In order to flatten the field, each cell would have to be tuned back to its original resonant frequency. However, significant correction can be achieved by shaping only the end cells and an optimising algorithm was written for such tuning.

3. SIMULATIONS

A single cavity as well as an entire 9-cell structure was modelled in two eigensolvers: HFSS (ver. 11.1) and Poisson Superfish (ver. 7.18). The 9-cell structure included beam pipes and modified end cells with increased iris size. [6]

In Superfish, an iris-to-iris geometry requires two electric planes as boundary conditions for a 0 mode and two magnetic planes for a π mode. Also, one magnetic and one electric plane produce a half- π mode. However, the cavity was drawn from one of the equators to the next (see Appendix) which meant that two electric planes could be used to find both 0 and π modes (see Fig. 3). The black dot indicates the drive point which should be placed in a region of high magnetic field. [7] More frequencies were found in HFSS by assigning master and slave boundary conditions and setting a required phase advance in the cell. Seven modes were found in each band, ranging from 0° to 180° in steps of 30° .

3.9 GHz 3rd Harmonic TESLA Cavity F = 3741.0885 MHz



3.9 GHz 3rd Harmonic TESLA Cavity F = 3900.0736 MHz

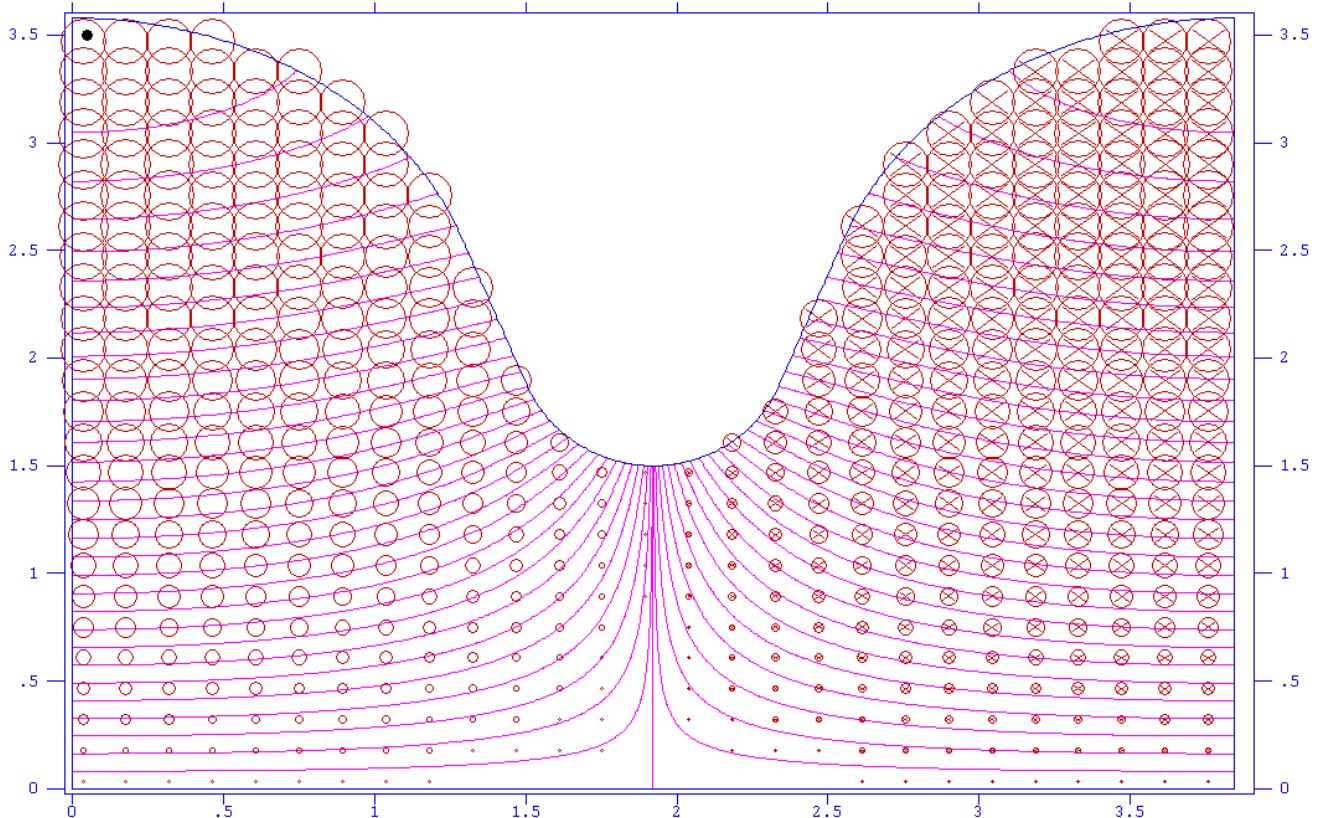


Figure 3: Electric field (lines) and magnetic field (circles) of a single cell of the XFEL Third Harmonic Cavity. H mode (lower) and 0 mode (upper) are shown.
Research conducted over the course of 7 weeks during the Summer of 2009. Accelerator Physics Note-01

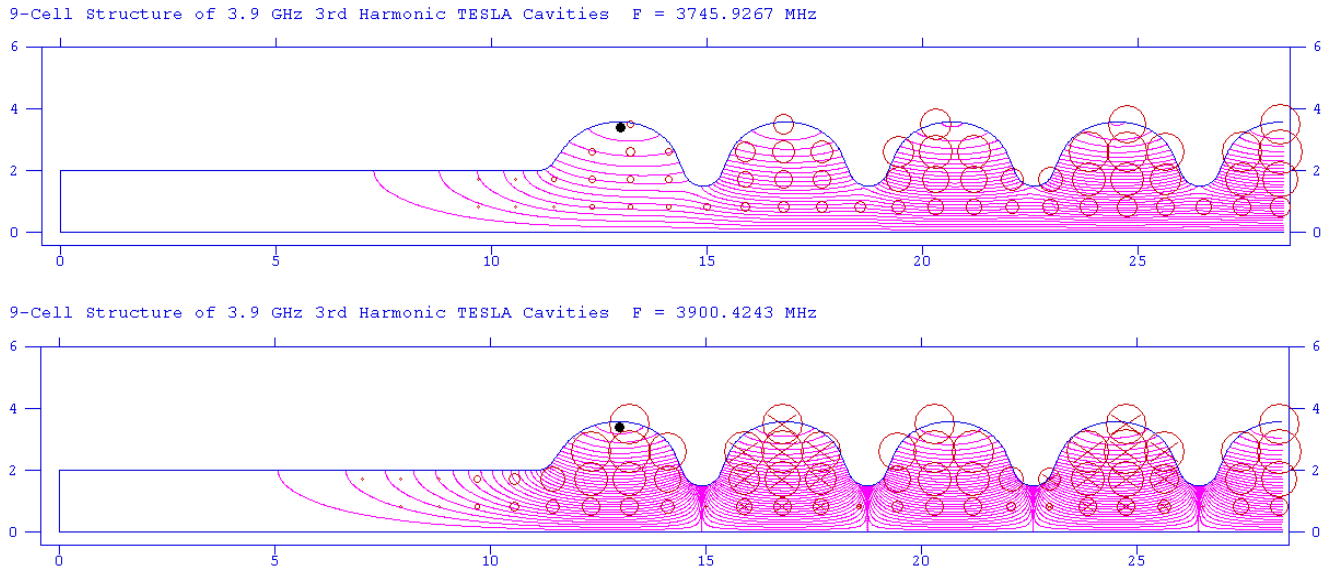


Figure 4: A 9-cell structure in 0 mode (upper) and π (lower) mode. Half of the structure shown.

Two sets of boundary conditions were employed when modelling a 9-cell structure with beam pipes and end cells. These were two electric and two magnetic planes. In this setup, phase advance had to be calculated from the field interpolated along at the axis of the cavity. [8]

Sensitivity to frequency deviations was tested by introducing random RMS errors of 1, 3 and 5 MHz to the resonant frequencies of the cavities. The optimising algorithm was then allowed to tune the frequency of end cells to obtain highest field flatness. The shifts required to flatten the field were calculated to the nearest 100 kHz as more accurate tuning is difficult in practice. [9]

4. RESULTS

Superfish simulations of a single cell did not result in identifying all of the expected 0 and π modes. However, modelling in HFSS returned all of these modes as well as the intermediate ones at 30° intervals. The data was then used to calculate the parameters characterising dispersion curves in first eight monopole bands. Long range coupling was extended to include three κ coefficients (see

Appendix). An average discrepancy between obtained analytical equations and the data from the simulations was less than 0.7% (see Fig. 5).

The simulations of the 9-cell structure showed a dependence on boundary conditions. The agreement between modes found with electric and magnetic planes exists only in the first band. Higher bands have frequencies above the cut-off of the beam pipes. The field enters the tubes and is affected by the boundary conditions assigned to the ends of the structure. However, the modes lie consistently on the dispersion curves (see Fig. 7) and both boundary conditions produce similar results in circuit model calculations (see Appendix).

The simulations of frequency errors were repeated 100 and 1000 times (see Fig. 8) for each error size and corresponding statistical data is given in Table 1 and 2 respectively. The effects of errors are reduced significantly even at large deviations from a 100% flatness. Figure 6 shows an example of a field profile before and after tuning. The flatness is more than doubled by changing the resonant frequencies by approx. 20 in the first cell and 10 MHz in the last cell.

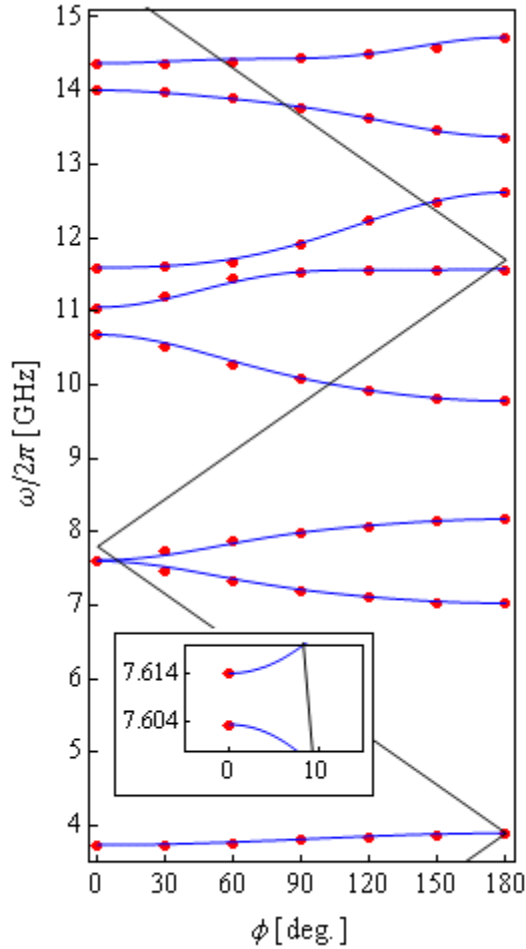


Figure 5: Single cell modes from simulations (red) with analytical dispersion curves from extended circuit model (blue). Second and third band are separated by approx. 10 MHz.

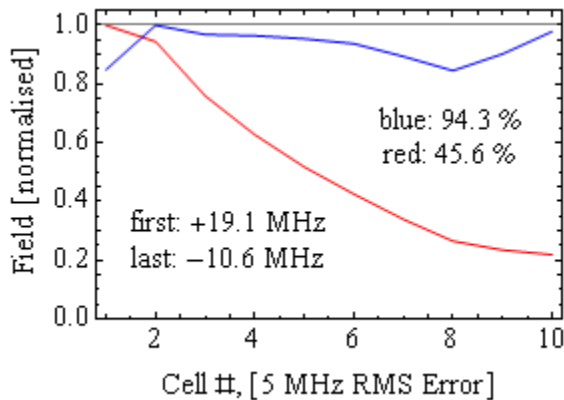


Figure 6: Field flatness correction with end cell tuning. Red line – with errors, blue – corrected. Tuning of the first and the last cell is indicated.

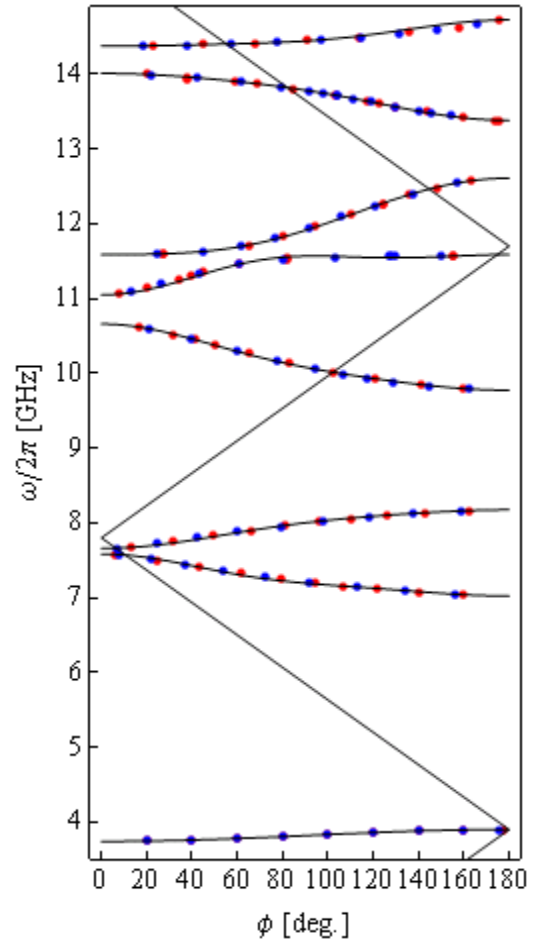


Figure 7: 9-cell modes from simulations with HH (red) and EE (blue) planes with analytical dispersion curves from extended circuit model.

Error [MHz]	FF before tuning [%]	FF after tuning [%]
1	93.6 ± 3.7	98.4 ± 0.6
3	81.0 ± 12.1	95.3 ± 1.8
5	69.3 ± 17.0	91.8 ± 3.2

Table 1: End cell tuning (100 simulations).

Error [MHz]	FF before tuning [%]	FF after tuning [%]
1	93.7 ± 3.8	98.3 ± 0.7
3	81.4 ± 10.8	95.0 ± 2.0
5	70.1 ± 16.4	91.7 ± 3.3

Table 2: End cell tuning (1000 simulations).

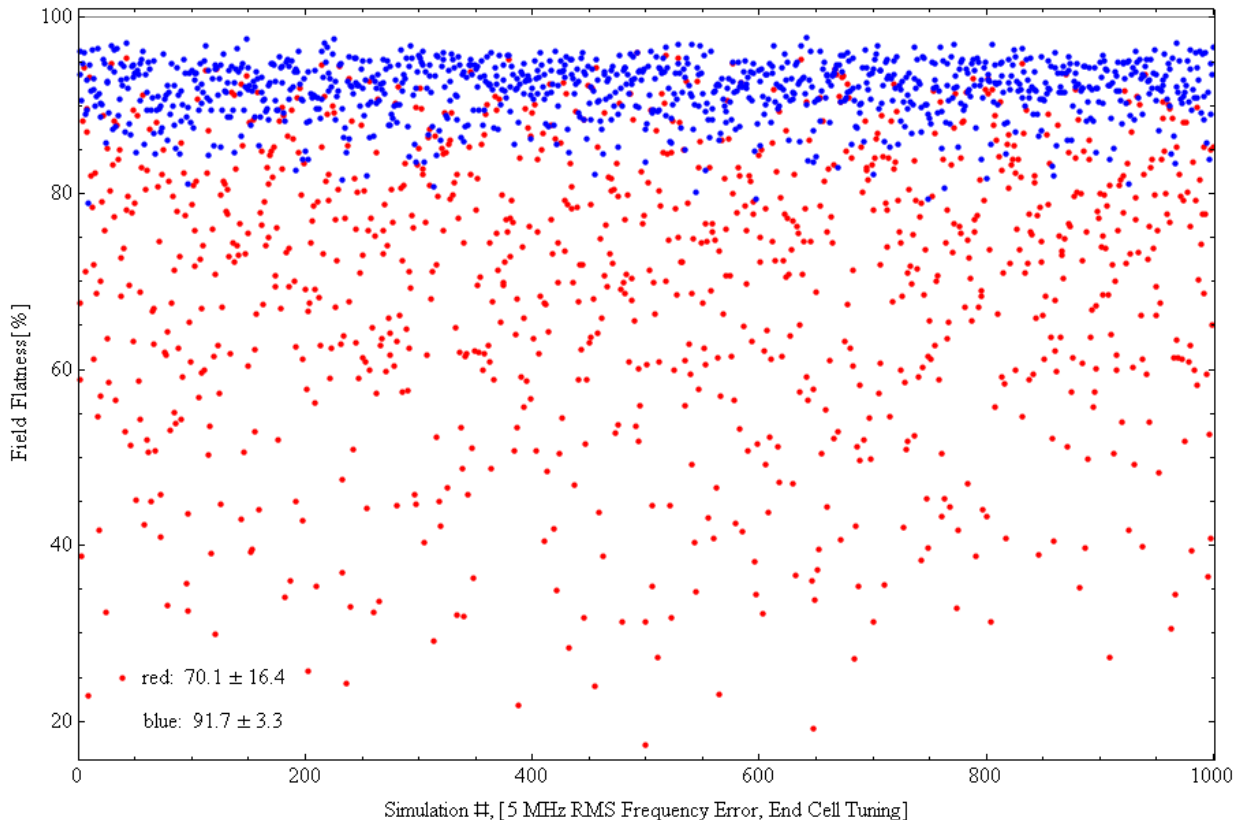


Figure 8: Result of 1000 simulations with 5MHz RMS error. Red – with errors, blue –corrected.

ACKNOWLEDGEMENTS

I would like to thank my supervisor Dr. R. M. Jones and his colleagues N. Juntong, V. Khan and Dr. I. Shinton for valuable advice provided during weekly meetings of the Manchester Electrodynamics and Wakefield (MEW) group at the Cockcroft Institute in Daresbury.

REFERENCES

- [1] R. M. Jones, 3.9 GHz Cavities at Flash, MEW Meeting, Cockcroft Institute, 25 June 2009.
- [2] T. I. Smith, proc linac acc conf '84, SLAC report **303**, pp. 421-425, 1986.
- [3] T. P. Wangler, RF Linear Accelerators, Wiley-VCH, 2nd ed., 2008.
- [4] H. Padamse, RF Superconductivity for Accelerators, Wiley-VCH, 2nd ed., 2008.
- [5] R. M. Jones, Linear Accelerators: Theory and Practical Applications: Week 3, Cockcroft Institute, 12 March – 22 April 2007.
- [6] T. Khabibouline et al, Higher Order Modes of a 3rd Harmonic Cavity with an Increased End-cup Iris, TESLA-FEL 2003-01, May 2003.
- [7] I. Shinton, Poisson Superfish tutorials, Cockcroft Institute and private communications.
- [8] R. Wanzenberg, Monopole, Dipole and Quadrupole Passbands of the TESLA 9-cell Cavity, TESLA 2001-33, September 2001.
- [9] R. M. Jones et al., Tuning and Field Sensitivity of Pi-mode Standing Wave Linacs for the NLC, SLAC-PUB-9247, EPAC 2002, Paris, France, 3 June – 7 June 2002.

APPENDIX

Poisson Superfish input file for a single cell:

(header for a field solving routine)

```
$reg kprob=1, ; SFish problem
dx=.02, ; mesh spacing
freq=3700.0, ; start in MHz
nbslo=1, ; lower b.c.
nbsup=1, ; upper b.c.
nbslf=1, ; left b.c.
nbsrt=0, ; right b.c.
icylin=1, ; cylin. coord.
xdri=.05,
ydri=3.5 $ ; drive point
```

(header for a frequency sweep)

```
... (starts as in field solving script)
freq=3700.0, ; start in MHz
delfr=0.5, ; step in MHz
nstep=10000, ; # of steps
nbslo=1, ; lower b.c.
... (continues as in field solving script)
```

(boundary points for a single cell)

```
$po x=0.0, y=0.0 $
$po x=0.0, y=3.5787 $
$po nt=2, x0=0.0, y0=2.0787,
a=1.36, b=1.50,
x=1.28433, y=0.49338 $
$po x=1.50694, y=1.86716 $
$po nt=2, x0=1.92167, y0=2.1,
a=0.45, b=0.60, x=0.0, y=-0.60 $
$po nt=2, x0=1.92167, y0=2.1,
a=0.45, b=0.60,
x=0.41473, y=-0.23284 $
$po x=2.55901, y=2.57208 $
$po nt=2,
x0=3.844334, y0=2.0787,
a=1.36, b=1.50, x=0.0, y=1.50 $
$po x=3.84334, y=0.0 $
$po x=0.0, y=0.0 $
```

Circuit model parameters of a single cell:

Band	f_r [GHz]	Δf [GHz]	$\Delta f / f_r$ [%]	κ_1 [%]	κ_2 [%]	κ_3 [%]
1	3.819	0.159	4.16	4.15	0.02	0.00
2	7.257	0.574	7.91	-7.42	-1.18	-0.32
3	7.935	0.560	7.06	6.80	1.43	0.38
4	10.115	0.901	8.89	-8.42	-1.11	-0.27
5	11.420	0.517	4.53	4.04	2.05	0.63
6	12.002	1.024	8.53	8.46	-1.18	-0.11
7	13.730	0.632	4.60	-4.38	0.72	-0.27
8	14.494	0.354	2.44	1.95	-0.74	0.46

Parameters of 9-cell structure (EE planes – left columns, HH planes – right columns):

Band	f_r [GHz]		Δf [GHz]		$\Delta f / f_r$ [%]		κ_1 [%]		κ_2 [%]		κ_3 [%]	
1	3.819	3.819	0.158	0.158	4.14	4.15	4.14	4.14	0.03	0.03	0.00	0.00
2	7.249	7.241	0.560	0.560	7.72	7.74	-7.11	-6.75	-1.10	-1.29	-0.45	-0.81
3	7.947	7.953	0.544	0.515	6.85	6.47	6.25	6.20	1.29	1.22	0.71	0.37
4	10.135	10.134	0.872	0.885	8.61	8.73	-8.18	-8.08	-0.99	-1.05	-0.26	-0.47
5	11.447	11.436	0.557	0.537	4.86	4.70	3.68	3.78	2.03	2.25	1.33	1.07
6	11.996	11.988	1.009	1.022	8.41	8.52	8.53	8.58	-1.18	-1.28	-0.30	-0.26
7	13.735	13.735	0.621	0.628	4.52	4.58	-4.37	-4.43	0.64	0.73	-0.18	-0.19
8	14.481	14.495	0.303	0.351	2.09	2.42	1.87	2.18	-0.64	-0.71	0.21	0.21